

Article

High-Temperature Rheological Properties of Asphalt Mortar Modified with Spent FCC Catalysts

Zhimei Wang, Lingyun Kong * and Shengqing He

School of Civil Engineering, Chongqing Jiaotong University, Chongqing 400074, China;
wangzhimei_cn@163.com (Z.W.); heshengqing2023@163.com (S.H.)

* Correspondence: konglingyun@cqjtu.edu.cn; Tel.: +86-23-62650387

Abstract: Spent fluid catalytic cracking catalysts (S-FCC-Cs) constitutes a fraction of the hazardous solid waste generated in the petrochemical industry. The resource application of S-FCC-Cs remains a challenge. This study aims to explore utilizing S-FCC-Cs in asphalt mortar as a means to enhance resource utilization. Five different S-FCC catalysts were used as substitutes for mineral powder in the asphalt slurry at varying proportions. The high-temperature rheology of the resulting spent FCC catalyst-modified asphalt slurry was analyzed using temperature scanning tests and multiple stress creep recovery (MSCR) tests conducted at different temperatures and substitution doping levels. As the proportion of alternative doping increased, both the phase angle and irrecoverable creep flexibility decreased, while the absolute values of the rutting factor, deformation recovery rate, and irrecoverable creep flexibility difference increased. Moreover, as the temperature rose, the phase angle increased while the rutting factor decreased. The inclusion of an alternative admixture significantly improved the high-temperature performance of the asphalt mastic. This improvement was attributed to several factors, including the increase in the elastic component, enhanced deformation resistance, and improved deformation recovery. While the high-temperature performance of spent FCC catalyst-modified asphalt mastic gradually declined with increasing test temperature, all performance indices remained superior to those of limestone mineral powder asphalt mastic. In addition, the asphalt mortar modified by S-FCC-C JX with a surface area and hydrophilic coefficient of $105\text{ m}^2/\text{g}$ and 1.026, respectively, exhibited the best rutting resistance and resilience performances among the five mortars, suggesting that the two factors co-affected the high-temperature rheological properties of S-FCC-C asphalt mortar. Considering stress sensitivity, it is more advantageous in improving the high-temperature deformation resistance of asphalt slurry at the JX dosage of 20%. These research findings offer valuable guidance for the application of S-FCC catalysts in asphalt pavement.



Citation: Wang, Z.; Kong, L.; He, S. High-Temperature Rheological Properties of Asphalt Mortar Modified with Spent FCC Catalysts. *Appl. Sci.* **2023**, *13*, 9376. <https://doi.org/10.3390/app13169376>

Academic Editor: Laurent Daudeville

Received: 28 May 2023

Revised: 5 August 2023

Accepted: 16 August 2023

Published: 18 August 2023



Copyright: © 2023 by the authors. Licensee MDPI, Basel, Switzerland. This article is an open access article distributed under the terms and conditions of the Creative Commons Attribution (CC BY) license (<https://creativecommons.org/licenses/by/4.0/>).

1. Introduction

Solid wastes, including industrial slags and construction waste, are valuable renewable resources [1]. After proper treatment, these materials can be effectively utilized in various applications such as bridges, dams, and airport roads [2–4]. Given the significant consumption of construction raw materials in road projects, and in line with global efforts to conserve energy, reduce emissions, and foster sustainable infrastructure, the field of road construction has emerged as a pivotal domain for the resourceful reuse of the aforementioned solid wastes.

Considerable research has been conducted both domestically and internationally on the application of solid waste in road construction. Tao et al. [2] incorporated steel slag as a mineral filler in asphalt mixes, resulting in improved deformation resistance and reduced low-temperature cracking of the asphalt binder. Skaf et al. [5] pre-treated electric furnace slag to replace a portion of the coarse aggregates and observed enhanced durability in

asphalt mixes. Extensive research has also been conducted on waste tire mastic powder-modified asphalt, focusing on modification mechanisms, production processes, and road performance [6,7]. As one kind of hazardous solid waste, the spent FCC catalysts (S-FCC-Cs) are generated in large quantities every year and are challenging to handle [8]. Some studies on the application of S-FCC-Cs exist in the field of catalysis, adsorption, construction, and others [9–13]. However, the application of S-FCC-Cs on an industrial scale is still limited. For instance, large-scale applications in urban fields or road engineering and so on [14–16].

FCC catalysts are complex mixtures that serve as catalytic reaction media formed through various physical and chemical reactions. They primarily consist of active substances, matrices, and binders [1,17,18], and are widely employed in the processing of petroleum light oil, during which certain raw materials are converted into coke. This coke leads to catalyst metal poisoning or pore blockage, resulting in the temporary deactivation of the active sites [18]. Consequently, a significant amount of spent catalysts with depleted activity precipitates. FCC spent catalysts contain heavy metal elements, such as Ni and V, which can be employed in the production of ceramics, bricks, and zeolites after appropriate treatment [19–23]. Alsheyab et al. [24,25] demonstrated that bituminous materials effectively immobilize heavy metals and radioactive elements. Moreover, the porous Y-type molecular sieve structure of FCC spent catalysts possesses a certain adsorption capacity. Hence, some studies [26–28] have proposed the substitution of spent FCC catalysts as fillers in asphalt mixtures, instead of mineral powder. Consequently, the utilization of spent FCC catalysts in asphalt mixtures can partially enhance the road performance of asphalt mixes.

A previous study proved that the mechanical and durable properties of asphalt mixtures are related to asphalt mortar. It is essential to study the variations of the properties of asphalt mixtures based on asphalt mortar's viscoelastic rheological properties [29]. For instance, Chen et al. [30] proved that the workability of asphalt mixtures is closely related to the viscoelastic properties of asphalt mortar based on dynamic shear rheological tests and digital image processing techniques. In addition, the high-temperature rheology of the asphalt binder pertains to the continuous strain and flow changes experienced by the binder over time after the application of a load. This property is closely associated with the high-temperature performance of an asphalt binder and can impact pavement issues such as rutting, waves, and undulations. Spent FCC catalysts exhibit a large specific surface area [31]. Consequently, when employed as fillers, they tend to adsorb more asphalt, thereby enhancing the high-temperature performance of the binder. Xue [32] analyzed the rheological properties of FCC catalysts and asphalt binders by examining their interaction. The study revealed that the addition of S-FCC catalysts to asphalt mastic increased the rutting factor, decreased the fatigue coefficient, improved high-temperature performance, and reduced low-temperature crack susceptibility. However, the existing study solely analyzed the effect of the powder-to-binder ratio on the high-temperature rheology of asphalt mortar, without addressing the impact of the substitution level of S-FCC-Cs for mineral powder on high-temperature rheology.

In this study, five S-FCC-Cs with different surface areas and hydrophilic coefficients were used as fillers to prepare five different asphalt mortars. The high-temperature rheological properties of these five asphalt mortars were investigated using a dynamic shear rheometer (DSR). The results showed that the dosage, surface area, and hydrophilic coefficients of S-FCC-Cs play key roles in the high-temperature rheological properties of asphalt mortar. The asphalt mortar based on S-FCC-C (JX) with a surface area and hydrophilic coefficient of $105\text{ m}^2/\text{g}$ and 1.016, respectively, exhibited the best rutting resistance and resilience performances among the five S-FCC-C asphalt mortars. To the best of our knowledge, this is the first study to investigate the high-temperature rheological properties of S-FCC-C asphalt mortar based upon both the temperature scan test and the multiple stress creep recovery (MSCR) test.

2. Experimental

2.1. Materials

Five S-FCC catalysts, namely JX, HC, LJ, SL, and ZH (Figure 1), were chosen as additives following appropriate treatment. These catalysts were acquired from Qingdao Huicheng Environmental Protection Technology Co. To assess their properties, the surface area, hydrophilic coefficient, and density of the S-FCC-C samples and mineral powder were measured in accordance with the guidelines outlined in a Chinese professional standard [33], titled “Test Procedure for Aggregates in Highway Engineering”. The results of these tests are presented in Table 1. The JX, LJ, SL, and ZH spent FCC catalysts are gray powders with a surface area of $100+ \text{ m}^2/\text{g}$. HC is a white powder with the lowest surface area and hydrophilic coefficient among the five catalysts, suggesting it has the greatest hydrophobicity. All the spent catalysts were used after metal ion leaching treatment to ensure that they were environmentally friendly.



Figure 1. The pictures of five S-FCC catalysts.

Table 1. Specific surface area, hydrophilicity coefficient, and density of FCC spent catalysts.

Raw Materials	Specific Surface Area (m^2/g)	Hydrophilic Coefficient	Density (g/m^3)
JX	105	1.016	2.630
HC	84	0.538	2.520
LJ	103	0.967	2.645
SL	117	1.124	2.485
ZH	109	0.700	2.689
Mineral powder	1.286	0.700	2.650

70# road petroleum asphalt was used as base asphalt (BA) in this work; its basic parameters are shown in Table 2.

Table 2. Basic parameters of the asphalt binder.

Technical Specifications	Unit	Test Results
Needle penetration (25°C)	0.1 mm	65.8
Needle penetration index PI	/	-1.2
Latency (10°C)	cm	25
Latency (15°C)	cm	>100
Softening point	$^\circ\text{C}$	47.5
Flash Point	$^\circ\text{C}$	320
Wax content	%	1.3
60 $^\circ\text{C}$ power viscosity	Pa.s	223
Density (15°C)	g/cm^3	1.04
Quality change	%	-0.33
Residual needle penetration ratio after TFOT	%	63.5
Residual latency (15°C)	cm	8.5

The mineral powder (MP) utilized in this study consists of limestone powder. The apparent density, water content, particle size range, and other technical parameters of the limestone powder comply with the applicable requirements outlined in a Chinese professional standard [34], titled “Technical Specification for Highway Asphalt Pavement Construction”.

2.2. Preparation of S-FCC-C-Modified Asphalt Slurry

First, the base asphalt was heated to a temperature of 150 °C for 1 h. Simultaneously, the mineral powder (MP) and S-FCC catalyst were heated to 165 °C for 1 h. Subsequently, the MP and the S-FCC-C (120 g) were blended at a temperature of 165 °C at varying weight ratios of W/W = 4/1, 3/2, 2/3, 1/4, and 0/1, corresponding to S-FCC-C dosages of 20%, 40%, 60%, 80%, and 100%. Finally, the hot base asphalt (100 g) was added to the mixture of MP/S-FCC in three separate batches, followed by a shearing process lasting 30 min at a temperature of 150 °C. The preparation process is visually depicted in Figure 2.

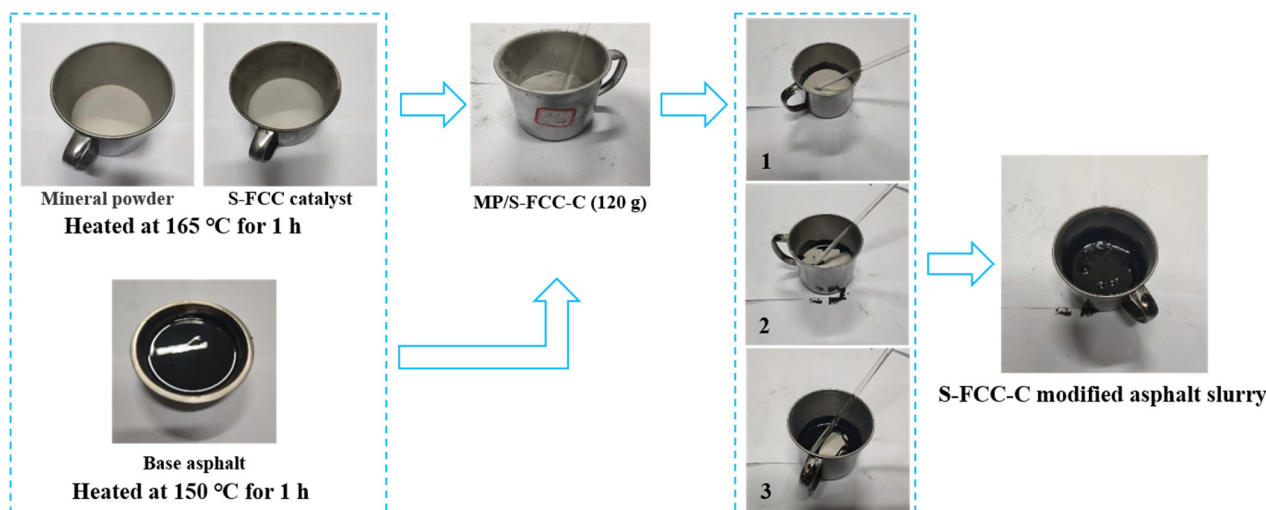


Figure 2. Preparation process of S-FCC-C-modified asphalt slurry. 1, 2, 3: the hot base asphalt was added to the MP/S-FCC in three separate batches.

2.3. Test Method

The characterization of the high-temperature rheological properties of asphalt mastics was conducted using a dynamic shear rheometer (DSR) for both the temperature scan test and the multiple stress creep recovery (MSCR) test. The instrument used for these tests was the Bohlin Gemini2 dynamic shear rheometer from Malvern Instruments. The experimental procedure is presented in Figure 3. All the tests were repeated three times, and the average values were obtained.

In the temperature scanning mode, the DSR provided data such as the phase angle (δ) and rutting factor ($G^*/\sin\delta$) to assess the high-temperature rheological properties of asphalt mastics. The phase angle (δ) serves as a relative indicator of the hysteresis behavior between the stress response and strain response of the asphalt slurry under oscillation. A larger phase angle indicates a more viscous asphalt slurry with a more pronounced hysteresis phenomenon. The rutting factor ($G^*/\sin\delta$) characterizes the resistance of the asphalt material to permanent deformation and reflects the high-temperature performance of the asphalt mastic. A higher rutting factor indicates greater elasticity of the asphalt slurry and stronger resistance to permanent deformation. The tests were conducted using a parallel plate with a 25 mm diameter and a 1 mm gap, spanning a temperature range of 30–80 °C; strain control mode was employed with an oscillation frequency of 10 rad/s and a strain amplitude of 12%. Results at 58 °C, 64 °C, 70 °C, and 76 °C were used to evaluate the high-temperature rheological properties of asphalt mastics.

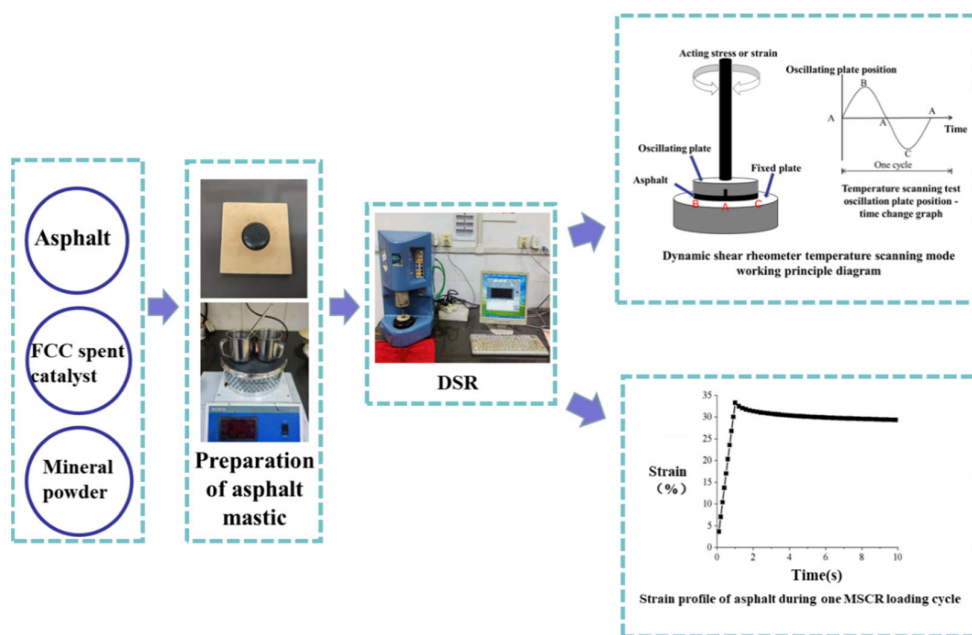


Figure 3. Schematic of the testing process. The rotation direction of the spin axis of DSR is A-B-A-C-A.

The MSCR test enabled the determination of the initial strain, residual strain, and total strain of each creep–recovery cycle at different stress levels. From these values, the irrecoverable creep flexibility (J_{nr}), irrecoverable creep flexibility difference ($J_{nr-diff}$), and deformation recovery rate (R) were calculated. R indicates the ability of asphalt to recover from deformation during creep, while J_{nr} represents irrecoverable deformation, and $J_{nr-diff}$ reflects the stress sensitivity of irrecoverable creep flexibility. A higher R value and a lower J_{nr} value signify easier recovery of asphalt deformation at high temperatures and better performance under such conditions. The tests were performed under stress levels of 0.1 and 3.2 kPa. Each creep–recovery cycle consists of 1 s of creep and 9 s of recovery, with the results of the last ten cycles being used for analysis. The test temperature chosen for this study was 60 °C. The calculations for R , J_{nr} , and $J_{nr-diff}$ are as follows [35]:

$$R = \frac{\varepsilon_c - \varepsilon_r}{\varepsilon_c - \varepsilon_o} \quad (1)$$

$$J_{nr} = \frac{\varepsilon_r - \varepsilon_o}{\tau} \quad (2)$$

$$J_{nr-diff} = \frac{(J_{nr3.2} - J_{nr0.1})}{J_{nr0.1}} \times 100\% \quad (3)$$

where ε_c , ε_r , ε_o , and τ are peak strain, residual deformation, initial strain, and stress levels during each loading cycle, respectively.

3. Results and Discussion

3.1. Temperature Scan Test Results

The phase angle (δ) obtained from the temperature scan test conducted using the dynamic shear rheometer is an effective indicator for characterizing the rheological properties of asphalt slurry [36]. Figure 4 illustrates the trend of the phase angle of the asphalt slurry with increasing S-FCC-C replacement admixture under different high-temperature conditions. The results indicate a general decrease in the phase angle as a result of FCC spent catalyst doping at the temperatures of 58 °C, 64 °C, 70 °C, and 76 °C employed in the experiment. This decrease suggests that the addition of S-FCC-Cs enhances the elastic component of the asphalt mastic while reducing the viscous component. The filler's

abundant specific surface area enables greater asphalt adsorption, resulting in a larger surface area interacting with the asphalt, a thinner asphalt film, a higher percentage of structural asphalt, and a lower percentage of free asphalt. Consequently, the phase angle tends to decrease with an increasing S-FCC-C replacement admixture, leading to an overall improved stability of the asphalt mastic [37,38]. However, certain test groups exhibited an increase in the phase angle at 20% and 60% replacement doping. For instance, at 64 °C, the phase angle of the asphalt mastic increased with 20% HC replacement doping, and at 76 °C, it increased with 60% SL replacement doping. This phenomenon can be attributed to the fact that the asphalt slurry material itself is a multi-phase material with inherent heterogeneity, resulting in a more intricate phase angle–change curve [39]. In specific cases, such as JX at 76 °C with 80% alternative doping and ZH at 58 °C with 80% alternative doping, a substantial increase in the phase angle was observed. Apart from potential test errors associated with the asphalt slurry itself, this increase can be attributed to the excessively large surface area of the filler relative to the amount of asphalt. In such cases, the surface of the filler particles may not be sufficiently conducive to forming a strong asphalt film, leading to reduced cohesion of the asphalt mastic, decreased overall strength, and an increase in the phase angle [40].

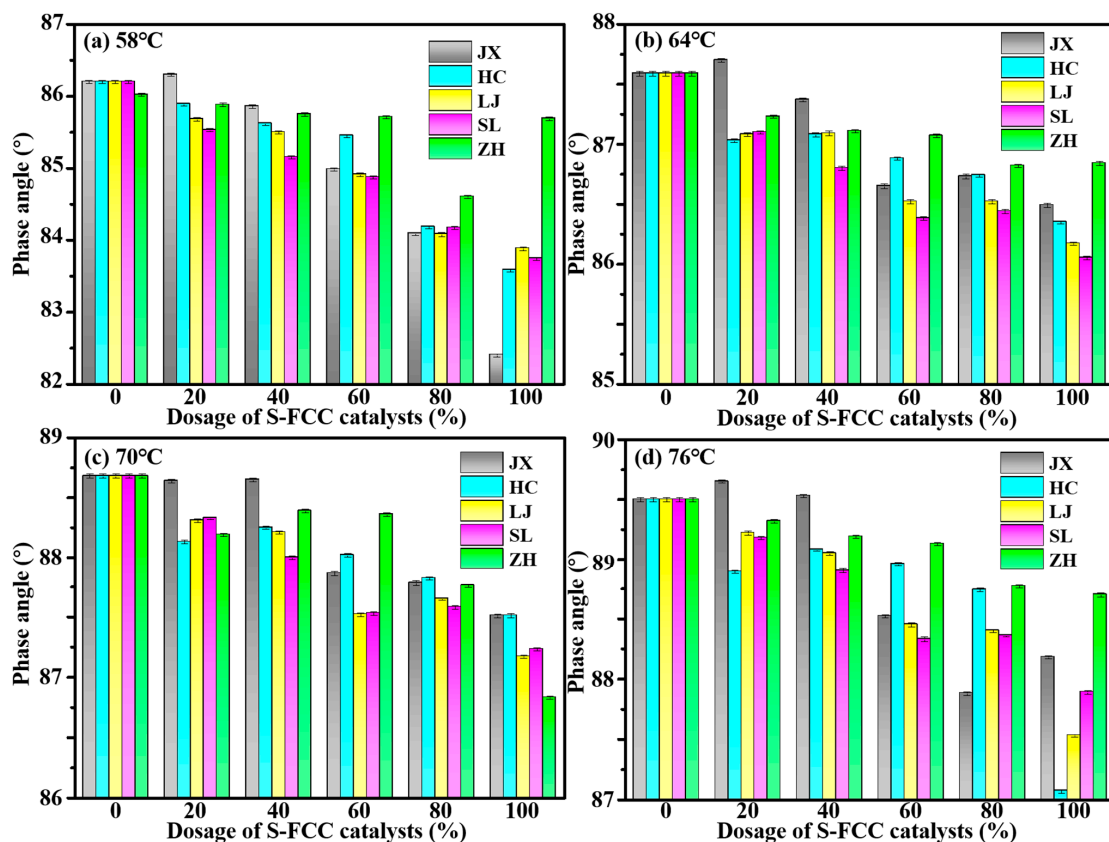


Figure 4. Change diagram of the phase angle of S-FCC catalyst-modified asphalt slurry at different temperatures.

To investigate the influence of high temperature on the rheological properties of asphalt mortar with different S-FCC-C substitution doses, the phase angle variation trend of S-FCC-C-modified asphalt slurry with temperatures at various doping levels was analyzed, as presented in Figure 5. From the figure, it can be observed that except for JX at 80% substitution dose and HC at 100% substitution dose, the phase angles consistently increased as the temperature rose from 58 °C to 76 °C. This shift indicates that the asphalt mastic gradually transitioned into a more viscous state, and the elevated temperatures adversely affected the internal structure of the modified asphalt mastic, leading to reduced stability. Notably,

the rising phase angles of the two aforementioned samples indicate a deviation from the overall trend, potentially attributed to specific characteristics of their compositions [41]. In general, the phase angles of the five S-FCC-C modified asphalt slurries were smaller when compared to those of the pure mineral powder asphalt slurry, with a more pronounced effect observed at higher S-FCC-C admixture levels. This phenomenon suggests that the inclusion of S-FCC-Cs resulted in a thinner asphalt film on the powder's surface within the asphalt mastic, particularly with increased doping amounts. Consequently, the structural asphalt content was higher, resulting in enhanced overall strength of the mastic.

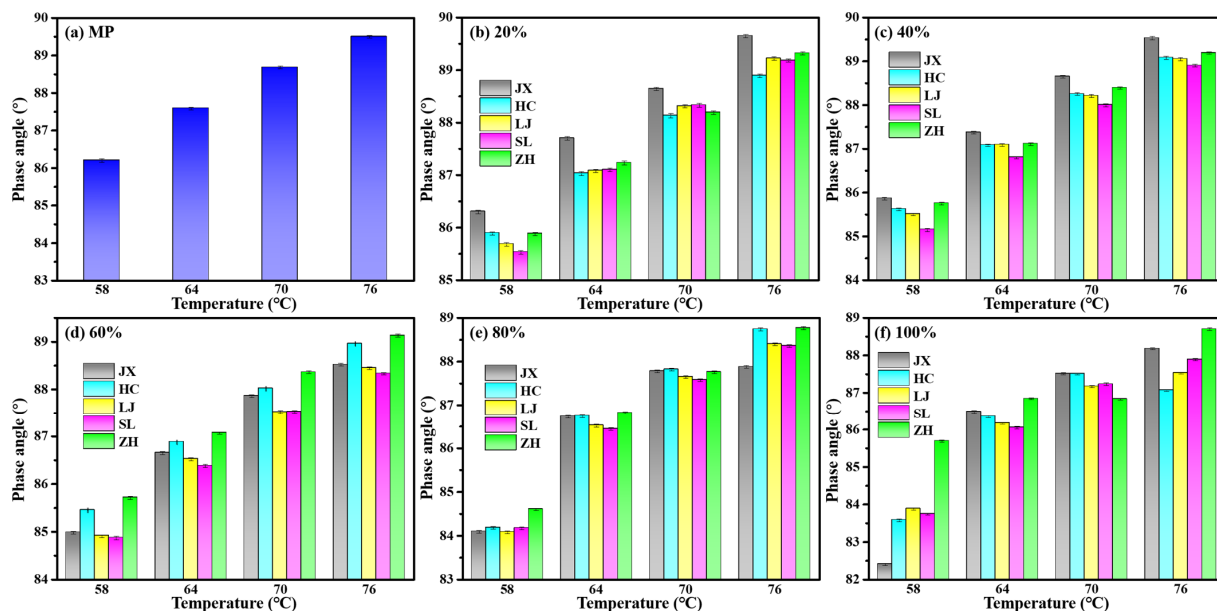


Figure 5. Phase angle-temperature change diagram of S-FCC catalyst-modified asphalt mortar with different dosages.

The rutting factor $G^*/\sin\delta$ obtained from the test provides an accurate assessment of the asphalt mastic's resistance to permanent deformation. A higher rutting factor indicates improved resistance to permanent deformation and better high-temperature performance of the asphalt mastic [42]. Figure 6 illustrates the trend of the rutting factor in S-FCC-C-modified asphalt slurry at different temperatures with varying admixture. Evidently, at the same temperature, the rutting factor of S-FCC-C-modified asphalt slurry shows significant improvement compared to limestone mineral powder asphalt slurry. Moreover, the rutting factor of different types of S-FCC-C-modified asphalt slurry increases with higher levels of alternative admixture. Incorporating an S-FCC-C admixture effectively enhances the high-temperature deformation resistance of the asphalt slurry. However, the modification effect of different types of S-FCC-Cs varies at different dosage levels. For instance, at 70 °C, the growth rates of JX, SL, LJ, HC, and ZH in the range of 20–40% alternative doping were 29.42%, 28.16%, 21.25%, 14.39%, and 8.24%, respectively. The modification effect ranking was as follows: JX > SL > LJ > HC > ZH. Notably, the modification effects of SL and LJ did not significantly differ within the 20–80% alternative doping range.

Figure 7 presents the rutting factor of S-FCC-C-modified asphalt mastic at different dosing levels with respect to temperature. The rutting factor of S-FCC-C-modified asphalt mastic decreases as the temperature increases, and the rate of decrease gradually diminishes. This indicates that the addition of different types of S-FCC-Cs enhances the high-temperature deformation resistance of the asphalt mastic to varying degrees, particularly during the initial stages of the test. The most substantial decrease in the rutting factor of S-FCC-C-modified asphalt mastic occurs between 58 °C and 64 °C, after which the rate of decrease gradually slows down. Furthermore, as the temperature reaches 76 °C and above, the rutting factor of different types of S-FCC-C-modified asphalt mastic gradually

converges to a similar level. In addition, the JX asphalt mortar exhibited the best rutting resistance ability among the five S-FCC-C asphalt mortars. This may be because the high surface area of JX allows it to adsorb more asphalt, while weak interaction of JX-to-asphalt (hydrophilic coefficient = 1.016) leads to the movement of asphalt on JX, resulting in the JX being the direct receptor of stress [43].

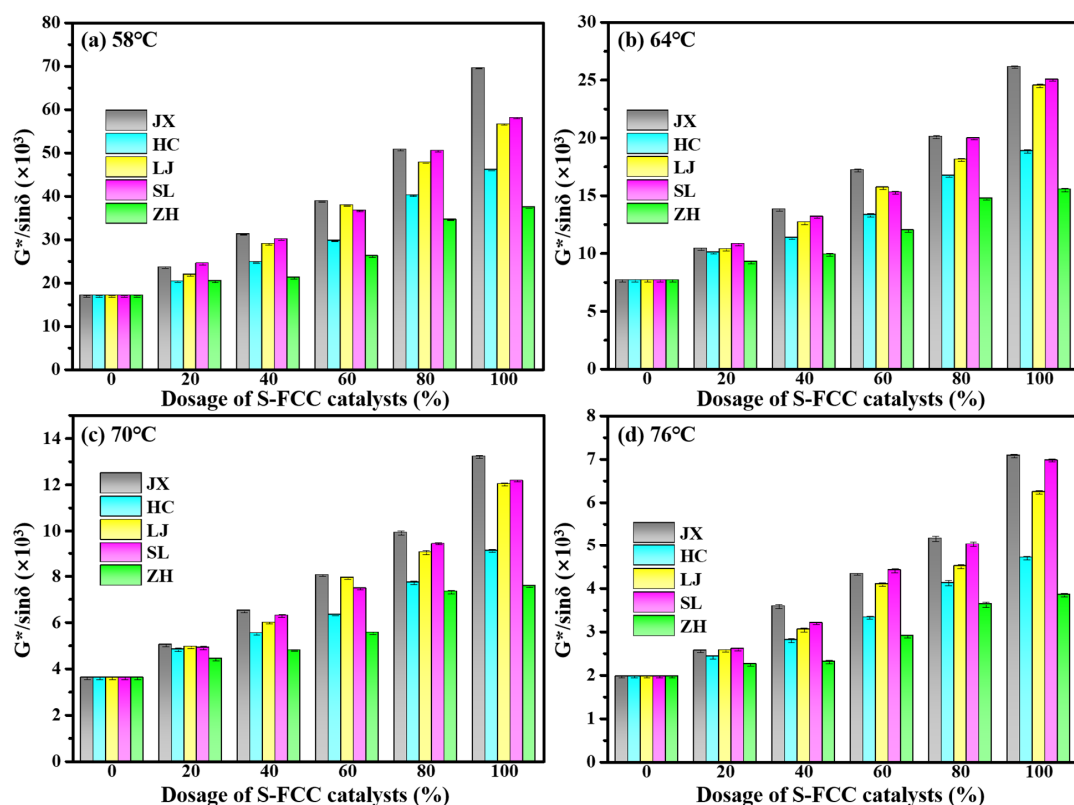


Figure 6. Rutting factor of S-FCC catalyst-modified asphalt mortar at different temperatures—change diagram of mixing amount.

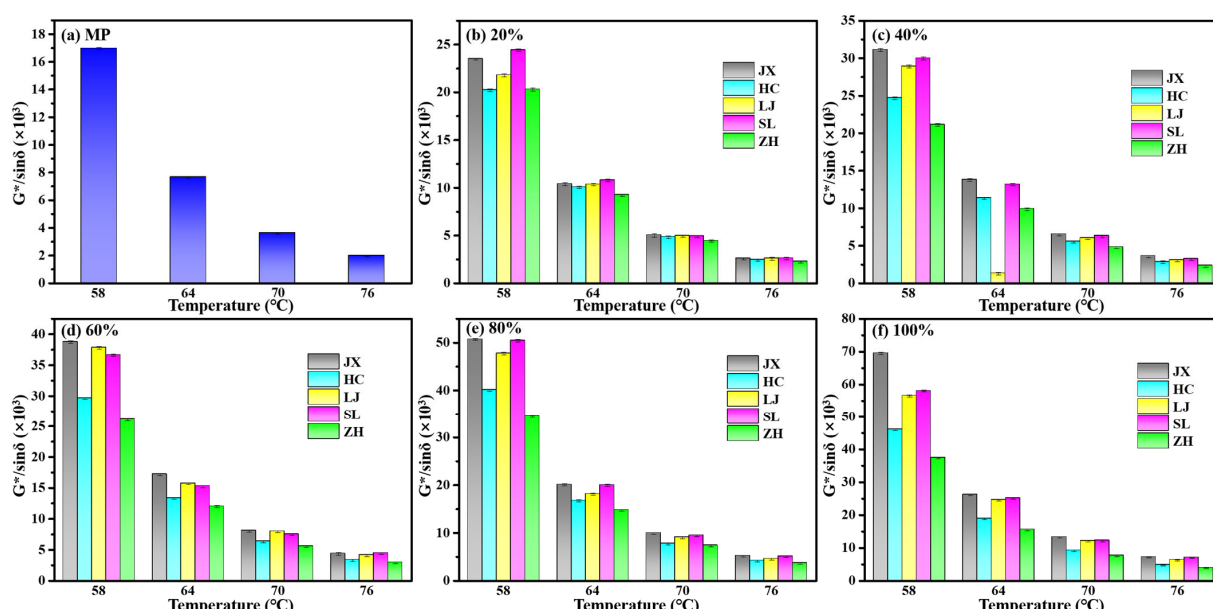


Figure 7. Rutting factor-temperature change diagram of S-FCC catalyst-modified asphalt mortar with different dosages.

3.2. MSCR

Figure 8 illustrates the correlation between the doping amount of S-FCC-Cs in the five FCC waste catalyst-modified asphalt mastics and the deformation recovery rates $R_{0.1}$ and $R_{3.2}$ under test conditions of 0.1 kPa and 3.2 kPa at 60 °C. From Figure 8, it can be observed that the deformation recovery rate R of S-FCC-C-modified asphalt mastic generally increases as the doping amount of S-FCC-Cs increases. This indicates that the overall resilience performance of S-FCC-C-modified asphalt mastic improves with higher levels of alternative doping, resulting in a higher percentage of deformation recovery. Under both stress conditions, the majority of S-FCC-C-modified asphalt mastics exhibited a marked increase in the growth rate of resilient energy at 80% doping, indicating a significant increase in the amount of structural asphalt adsorbed by S-FCC-Cs at high doping levels. This conversion led to a greater proportion of viscous components in the asphalt mastic being transformed into elastic components, resulting in a significant improvement in high-temperature performance. Interestingly, the $R_{3.2}$ value of JX asphalt mortar increased sharply with the increase in JX dosage, indicating the excellent deformation recovery ability of JX asphalt mortar. It was found that there was a slight phase separation phenomenon that appeared in the JX asphalt mortar during the experiment. The phase separation of JX from the asphalt may lead to the movement of asphalt on JX, which should be the reason that the JX asphalt mortar exhibited the best resilience among the five asphalt mortars under the stress of 3.2 kPa.

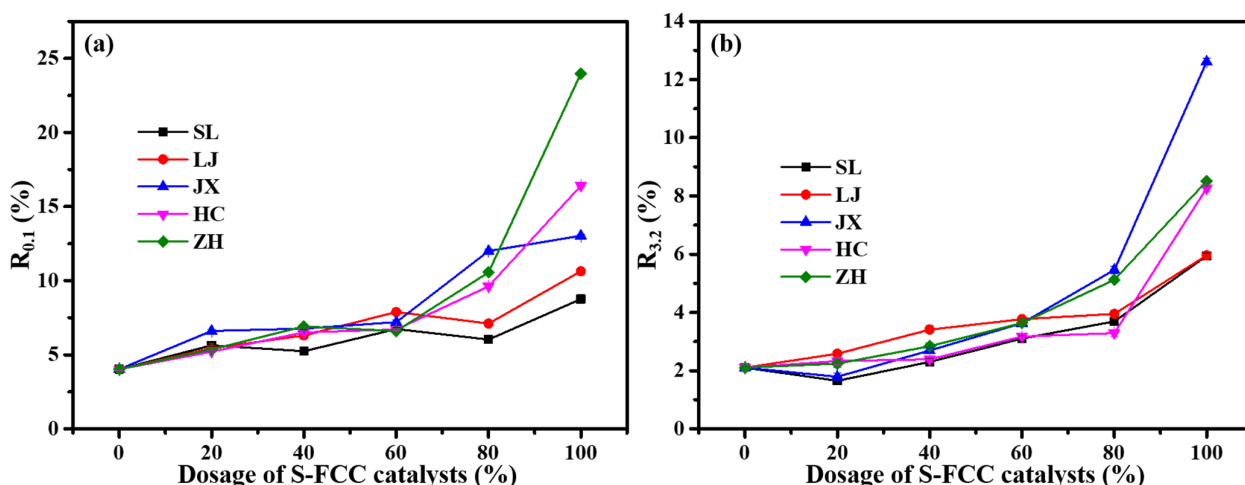


Figure 8. Variation in deformation recovery rate R tested under 0.1 kPa (a) and 3.2 kPa (b) of S-FCC catalyst-modified asphalt mortar with dosage.

$J_{nr}(0.1/3.2)$ was polynomially fitted, and the corresponding fitted curves and functions are presented in Figure 9, along with the detailed results in Tables 3 and 4. Figure 9 displays the graphical representation of the average irrecoverable creep flexibility, $J_{nr0.1}$ and $J_{nr3.2}$, as they vary with the S-FCC-C admixture levels in the five FCC spent catalyst-modified asphalt mastics at 60 °C.

Table 3. Fitting formula for the change in $J_{nr0.1}$ of S-FCC-C-modified asphalt mortar with the dosage.

Powder Type	$J_{nr}(0.1)$ and Doping Fitting Function	R^2
ZH	$y = 0.68786 - 0.00661x + 0.0000982143x^2$	0.970
LJ	$y = 0.65214 - 0.00833x + 0.0000330357x^2$	0.990
SL	$y = 0.64214 - 0.00840x + 0.0000348214x^2$	0.983
JX	$y = 0.64964 - 0.01124x + 0.0000611607x^2$	0.992
HC	$y = 0.63679 - 0.00690x + 0.0000254464x^2$	0.961

Table 4. Fitting formula for the change in $Jnr_{3.2}$ of S-FCC-C-modified asphalt mortar with the dosage.

Powder Type	$Jnr_{(3.2)}$ with Doping Fitting Function	R^2
ZH	$y = 0.50214 - 0.00629x + 0.0000151786x^2$	0.978
LJ	$y = 0.49893 - 0.00741x + 0.0000299107x^2$	0.993
SL	$y = 0.53643 - 0.00730x + 0.0000241071x^2$	0.968
JX	$y = 0.51536 - 0.00905x + 0.0000415179x^2$	0.995
HC	$y = 0.50179 - 0.00710x + 0.0000281250x^2$	0.984

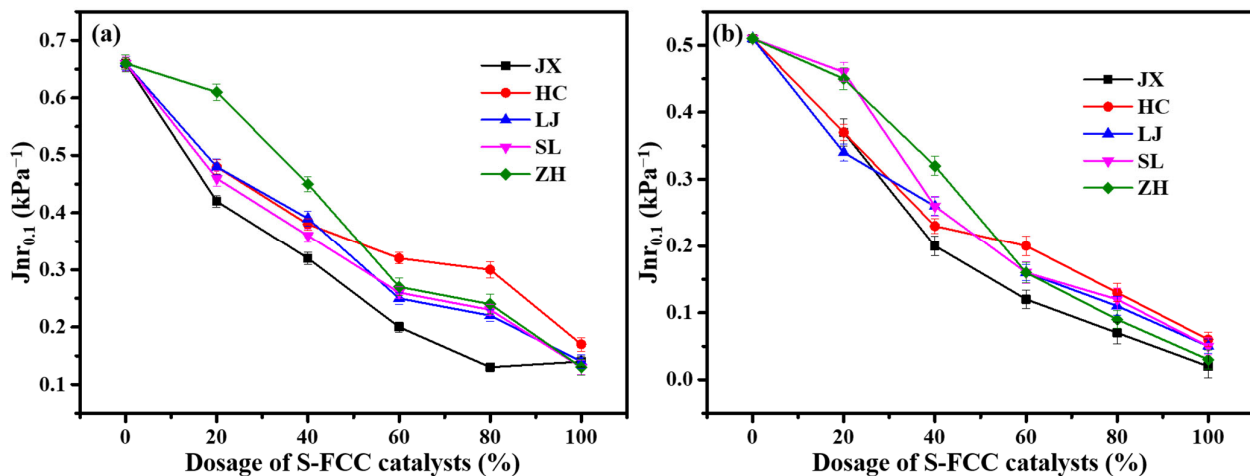
**Figure 9.** Diagram of unrecoverable creep modulus Jnr tested under 0.1 kPa (a) and 3.2 kPa (b) of S-FCC-C-modified asphalt mortar with dosage.

Figure 9 indicates a well-fitted quadratic function between the irrecoverable creep flexibility of S-FCC-C-modified asphalt mastic and the S-FCC-C alternative doping, with an R^2 value exceeding 0.9. The irrecoverable creep flexibility gradually decreases with increasing S-FCC-C doping, and the slope of the curve decreases accordingly. This indicates that the incorporation of S-FCC-Cs enhances the resistance to permanent deformation and improves the high-temperature performance of the asphalt mastic, with a more pronounced effect at higher doping levels. At lower doses, the variation in the S-FCC-Cs dosage has a significant impact on the Jnr of the asphalt slurry, whereas at higher doses, the influence becomes less pronounced. Increasing the replacement dosage of the FCC spent catalyst significantly enhances the high-temperature performance of the asphalt slurry at lower doses, but the effect gradually diminishes at higher doses. Furthermore, it can be seen from Figure 9 that the Jnr value of JX asphalt mortar is higher than that of the other four, which is consistent with the rutting factor results.

Figure 10 presents the absolute value of the irrecoverable creep flexibility difference, $Jnr\text{-diff}$, plotted against the S-FCC-Cs replacement doping.

In the current experimental study, it was observed that $Jnr_{0.1}$ was higher than $Jnr_{3.2}$ regardless of the presence or absence of S-FCC-Cs substitution. This finding contrasts with conventional MSCR test results for asphalt materials. Consequently, negative values of $Jnr\text{-diff}$ were calculated for all test groups. Further investigation of the relevant literature revealed that such results are attributed to the filler volume filling-effect resulting from the filler ratio [43,44]. In asphalt mastics with a lower powder content, the load is primarily borne by the asphalt component under both low- and high-stress conditions. Under high-stress conditions, this leads to a greater cumulative strain and a larger Jnr value and hence, a positive $Jnr\text{-diff}$ value. In asphalt mastics with a higher powder content, as the filler assumes the role of the main load-bearing component under high-stress conditions, the interaction between the powder particles causes a significantly smaller strain in the creep phase and residual strain in the recovery phase compared to when the asphalt is the primary load-bearing component. Consequently, the Jnr value decreases accordingly, leading to

negative Jnr-diff values. The higher the percentage of S-FCC-Cs in the mixed filler, the more pronounced the overall filling effect of the filler and the greater the stress sensitivity.

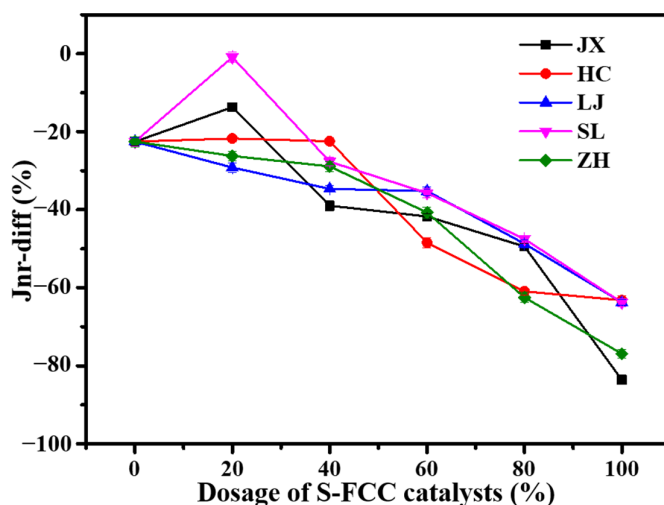


Figure 10. Jnr-diff relationship between the replacement amount of S-FCC catalyst and the irrecoverable creep compliance difference at 60 °C.

As depicted in Figure 10, at a 20% admixture, the absolute Jnr-diff values of different types of FCC spent catalyst-modified asphalt mastics exhibit varying increases and decreases compared to mineral powder asphalt mastics. This suggests that at lower dosage levels, different FCC waste catalysts exert varying degrees of influence on the filling effect of S-FCC-C/MP mixed filler. HC, SL, and JX S-FCC-C reduce the stress sensitivity of the asphalt mastic when replacing 20% mineral powder. However, as the replacement amount further increases, the filling effect gradually becomes stronger than that of mineral powder asphalt mastic, resulting in increased stress sensitivity. Thus, from a stress sensitivity perspective, HC, SL, and JX are more advantageous in improving the high-temperature deformation resistance of asphalt slurry at lower dosages.

4. Conclusions

- (1) At the same test temperature, the phase angle of S-FCC-C-modified asphalt slurry decreases, and the rutting factor increases with an increase in the S-FCC-C replacement dose, leading to a significant enhancement in the high-temperature performance of the modified asphalt slurry.
- (2) With the same dose, the phase angle of the S-FCC-C-modified asphalt slurry increases, and the rutting factor decreases as the test temperature rises. This results in a decrease in the high-temperature performance of the modified asphalt slurry, although it remains superior to limestone powder asphalt slurry.
- (3) The deformation recovery rates $R_{0.1}$ and $R_{3.2}$ increase as the S-FCC-C replacement admixture increases, leading to a substantial improvement in high-temperature performance, particularly at an 80% replacement admixture. Meanwhile, the average non-recoverable creep flexibilities $Jnr_{0.1}$ and $Jnr_{3.2}$ decrease, with a higher decrease rate observed at low dosing compared to high dosing. This signifies a significant enhancement in the recovery deformation capacity of the asphalt mastic at low S-FCC-C dosing, which gradually diminishes at higher dosing.
- (4) The alternative admixture of S-FCC-C enhances the filling effect of the filler in the asphalt mastic, resulting in a reversed increase in stress sensitivity at higher admixtures (negative Jnr-diff values). A 20% alternative admixture of HC, SL, and JX samples improves the stress sensitivity of mineral powder asphalt mastic. Therefore, 20% represents the optimal alternative admixture for HC, SL, and JX samples.

- (5) The asphalt mortar filled with JX exhibited the best rutting resistance and resilience performance among the five S-FCC-C asphalt mortars, suggesting that the surface area and hydrophilic coefficient of S-FCC-Cs co-affect the high-temperature rheological performance of asphalt mortar. Considering stress sensitivity, the use of JX can be recommended to replace 20% of mineral powder in the aggregate in the pavement construction.

Author Contributions: Methodology, investigation, data curation, and writing—original draft preparation, Z.W. and S.H.; writing—review and editing, supervision, and funding acquisition, L.K. All authors have read and agreed to the published version of the manuscript.

Funding: This research was funded by the Science and Technology Plan Project of Chongqing Transportation Bureau, grant number CQJT2022ZC09.

Institutional Review Board Statement: Not applicable.

Informed Consent Statement: Not applicable.

Data Availability Statement: Not applicable.

Conflicts of Interest: The authors declare no conflict of interest.

References

- Vishnu, T.B.; Singh, K.L. A study on the suitability of solid waste materials in pavement construction: A review. *Int. J. Pavement Res. Technol.* **2020**, *14*, 625–637. [[CrossRef](#)]
- Tao, G.; Xiao, Y.; Yang, L.; Cui, P.; Kong, D.; Xue, Y. Characteristics of steel slag filler and its influence on rheological properties of asphalt mortar. *Constr. Build. Mater.* **2019**, *201*, 439–446. [[CrossRef](#)]
- Li, C.; Wang, H.; Fu, C.; Shi, S.; Liu, Q.; Xu, P.; Liu, Q.; Zhou, D.; Cheng, Y.; Jiang, L. Effect and mechanism of waste glass powder silane modification on water stability of asphalt mixture. *Constr. Build. Mater.* **2023**, *366*, 130086. [[CrossRef](#)]
- Zheng, Y.; Chen, S.; Huang, W.; Cai, X.; Huang, J.; Wu, K. Principle analysis of the mix design and performance evaluation of the asphalt-filler volume equivalent substitution method. *Constr. Build. Mater.* **2023**, *367*, 130276. [[CrossRef](#)]
- Skaf, M.; Manso, J.M.; Aragón, Á.; Fuente-Alonso, J.A.; Ortega-López, V. EAF slag in asphalt mixes: A brief review of its possible reuse. *Resour. Conserv. Recycl.* **2017**, *120*, 176–185. [[CrossRef](#)]
- Hamzani; Munirwansyah; Hasan, M.; Sugiarto, S. Determining the properties of semi-flexible pavement using waste tire rubber powder and natural zeolite. *Constr. Build. Mater.* **2021**, *266*, 121199. [[CrossRef](#)]
- Wang, Q.; Wang, N.; Tseng, M.; Huang, Y.; Li, N. Waste tire recycling assessment: Road application potential and carbon emissions reduction analysis of crumb rubber modified asphalt in China. *J. Clean. Prod.* **2020**, *249*, 119411. [[CrossRef](#)]
- Ferella, F.; Innocenzi, V.; Maggiore, F. Oil refining spent catalysts: A review of possible recycling technologies. *Resour. Conserv. Recycl.* **2016**, *108*, 10–20. [[CrossRef](#)]
- Kanduri, K.P.; Seethamraju, S. Effect of process mode on product yields and selectivity in the catalytic co-pyrolysis of peanut shells and polypropylene using spent fluid catalytic cracking (FCC) catalyst. *Bioresour. Technol. Rep.* **2023**, *22*, 101478. [[CrossRef](#)]
- Mavukwana, A.; Burra, K.G.; Sempuga, C.; Castaldi, M.; Gupta, A.K. Effect of spent fluid catalytic cracking (FCC) catalyst on syngas production from pyrolysis and CO₂-assisted gasification of waste tires. *Fuel* **2024**, *355*, 129446. [[CrossRef](#)]
- Su, B.; Shi, L.; Meng, X.; Wang, X.; Liu, N. From waste to best: Excellent desulfurization performance of spent FCC catalyst. *J. Sulfur Chem.* **2019**, *40*, 75–87. [[CrossRef](#)]
- Al-Jabri, K.; Baawain, M.; Taha, R.; Al-Kamyani, Z.S.; Al-Shamsi, K.; Ishtieh, A. Potential use of FCC spent catalyst as partial replacement of cement or sand in cement mortars. *Constr. Build. Mater.* **2013**, *39*, 77–81. [[CrossRef](#)]
- Velázquez, S.; Monzó, J.; Borrachero, M.V.; Soriano, L.; Payá, J. Evaluation of the pozzolanic activity of spent FCC catalyst/fly ash mixtures in Portland cement pastes. *Thermochim. Acta* **2016**, *632*, 29–36. [[CrossRef](#)]
- Liu, C.; Cui, J.; Zhang, Z.; Liu, H.; Huang, X.; Zhang, C. The role of TBM asymmetric tail-grouting on surface settlement in coarse-grained soils of urban area: Field tests and FEA modelling. *Tunn. Undergr. Space Technol.* **2021**, *111*, 103857. [[CrossRef](#)]
- Qiu, R.; Wang, W.; Wang, Z.; Wang, H. Advancement of modification engineering in lean methane combustion catalysts based on defect chemistry. *Catal. Sci. Technol.* **2023**, *13*, 2566–2584. [[CrossRef](#)]
- Alshamsi, K.; Baawain, M.; Aljabri, K.; Taha, R.; Al-kamyani, Z. Utilizing waste spent catalyst in asphalt mixtures. *Procedia Soc. Behav. Sci.* **2012**, *53*, 326–334. [[CrossRef](#)]
- Liu, H.; He, H.; Li, Y.; Hu, T.; Ni, H.; Zhang, H. Coupling effect of steel slag in preparation of calcium-containing geopolymers with spent fluid catalytic cracking (FCC) catalyst. *Constr. Build. Mater.* **2021**, *290*, 123194. [[CrossRef](#)]
- Tian, X.; Han, S.; Wang, K.; Shan, T.; Li, Z.; Li, S.; Wang, C. Waste resource utilization: Spent FCC catalyst-based composite catalyst for waste tire pyrolysis. *Fuel* **2022**, *328*, 125236. [[CrossRef](#)]
- Myrrin, V.; Pedroso, A.M.; Ponte, H.A.; Ponte, M.J.J.; Alekseev, K.; Evaniki, D.; Pan, R.C.Y. Thermal engineering method application for hazardous spent petrochemical catalyst neutralization. *Appl. Therm. Eng.* **2017**, *110*, 1428–1436. [[CrossRef](#)]

20. Taha, R.; Al-Kamyani, Z.; Al-Jabri, K.; Baawain, M.; Al-Shamsi, K. Recycling of waste spent catalyst in road construction and masonry blocks. *J. Hazard. Mater.* **2012**, *229–230*, 122–127. [[CrossRef](#)]
21. Basaldella, E.I.; Torres Sánchez, R.M.; Conconi, M.S. Conversion of exhausted fluid cracking catalysts into zeolites by alkaline fusion. *Appl. Clay Sci.* **2009**, *42*, 611–614. [[CrossRef](#)]
22. Chen, H.; Tseng, Y.; Hsu, K. Spent FCC catalyst as a pozzolanic material for high-performance mortars. *Cem. Concr. Compos.* **2004**, *26*, 657–664. [[CrossRef](#)]
23. Rodríguez, E.D.; Bernal, S.A.; Provis, J.L.; Gehman, J.D.; Monzó, J.M.; Payá, J.; Borrachero, M.V. Geopolymers based on spent catalyst residue from a fluid catalytic cracking (FCC) process. *Fuel* **2013**, *109*, 493–502. [[CrossRef](#)]
24. Alsheyab, M.A.T.; Khedaywi, T.S.; Elayan, M.S. Laboratory study on solidification/stabilization of unwanted medications using asphalt as a binder. *J. Mater. Cycles Waste Manag.* **2012**, *15*, 129–137. [[CrossRef](#)]
25. Cervinkova, M.; Vondruska, M.; Bednarik, V.; Pazdera, A. Stabilization/solidification of munition destruction waste by asphalt emulsion. *J. Hazard. Mater.* **2007**, *142*, 222–226. [[CrossRef](#)]
26. Furimsky, E. Spent refinery catalysts: Environment, safety and utilization. *Catal. Today* **1996**, *30*, 223–286. [[CrossRef](#)]
27. Schmitt, R. FCC catalyst finds three safe reuse outlets in Europe. *Oil Gas J.* **1991**, *89*, 46.
28. Wai, C.M.; Frye, J.G.; Fulton, J.L.; Bowman, L.E.; Silva, L.J.; Gerber, M.A. *Regeneration of Hydrotreating and FCC Catalysts*; Pacific Northwest National Lab (PNNL): Richland, WA, USA, 1999. [[CrossRef](#)]
29. Akisetty, C.; Xiao, F.; Gandhi, T.; Amirkhanian, S. Estimating correlations between rheological and engineering properties of rubberized asphalt concrete mixtures containing warm mix asphalt additive. *Constr. Build. Mater.* **2011**, *25*, 950–956. [[CrossRef](#)]
30. Dong, F.; Zu, Y.; Chen, B.; Yu, X.; Huang, J. Laboratory investigations of the effects of asphalt mortar and its viscoelasticity on the workability of asphalt mixtures. *Constr. Build. Mater.* **2023**, *389*, 131756. [[CrossRef](#)]
31. Lu, G.; Lu, X.; Liu, P. Reactivation of spent FCC catalyst by mixed acid leaching for efficient catalytic cracking. *J. Ind. Eng. Chem.* **2020**, *92*, 236–242. [[CrossRef](#)]
32. Xue, Y.; Wei, X.; Zhao, H.; Wang, T.; Xiao, Y. Interaction of spent FCC catalyst and asphalt binder: Rheological properties, emission of VOCs and immobilization of metals. *J. Clean. Prod.* **2020**, *259*, 120830. [[CrossRef](#)]
33. JTG E42-2005; Test Procedure for Aggregates in Highway Engineering. Chinese Professional Standard. Ministry of Transport of the People's Republic of China: Beijing, China, 2005.
34. JTG F40-2004; Technical Specification for Highway Asphalt Pavement Construction. Chinese Professional Standard. Ministry of Transport of the People's Republic of China: Beijing, China, 2004.
35. D'Angelo, J.; Dongré, R. Practical use of multiple stress creep and recovery test: Characterization of Styrene–Butadiene–Styrene dispersion and other additives in Polymer-Modified asphalt binders. *Transp. Res. Rec.* **2009**, *2126*, 73–82. [[CrossRef](#)]
36. Wang, N.; Li, C.; Xu, C. Effect of basalt fibers on rheological property of asphalt mortar. *Adv. Mater. Res.* **2015**, *1095*, 233–236. [[CrossRef](#)]
37. Liu, G.; Yang, T.; Li, J.; Jia, Y.; Zhao, Y.; Zhang, J. Effects of aging on rheological properties of asphalt materials and asphalt-filler interaction ability. *Constr. Build. Mater.* **2018**, *168*, 501–511. [[CrossRef](#)]
38. Cui, L.; Xu, J.; Cen, L.; Ren, M.; Cao, F. Molecular engineering and modification of FCC slurry oil residue for improving ageing resistance of high quality paving asphalt. *Constr. Build. Mater.* **2021**, *299*, 124234. [[CrossRef](#)]
39. Han, S.; Sun, P.; Fwa, T.F. Relationships between internal structure and surface texture of asphalt mixtures. *Road Mater. Pavement Des.* **2019**, *22*, 894–909. [[CrossRef](#)]
40. Harris, F.A. Asphalt membranes in expressway construction. *Transp. Res. Board Natl. Acad. Sci.* **1963**, *7*, 34–46.
41. Cao, K.; Xu, W.; Chen, D.; Feng, H. High-and low-temperature properties and thermal stability of silica fume/SBS composite-modified asphalt mortar. *Adv. Mater. Sci. Eng.* **2018**, *2018*, 1317436.
42. Ling, C.; Arshadi, A.; Bahia, H. Importance of binder modification type and aggregate structure on rutting resistance of asphalt mixtures using image-based multi-scale modelling. *Road Mater. Pavement Des.* **2016**, *18*, 785–799. [[CrossRef](#)]
43. Zulkati, A.; Diew, W.Y.; Delai, D. Effects of fillers on properties of asphalt-concrete mixture. *J. Transp. Eng. ASCE* **2012**, *138*, 902–910. [[CrossRef](#)]
44. Guo, M.; Bhasin, A.; Tan, Y. Effect of mineral fillers adsorption on rheological and chemical properties of asphalt binder. *Constr. Build. Mater.* **2017**, *141*, 152–159. [[CrossRef](#)]

Disclaimer/Publisher's Note: The statements, opinions and data contained in all publications are solely those of the individual author(s) and contributor(s) and not of MDPI and/or the editor(s). MDPI and/or the editor(s) disclaim responsibility for any injury to people or property resulting from any ideas, methods, instructions or products referred to in the content.